

# ***Monitoring and Controlling the Temperature in a High power Direct Diode Laser Surface Hardening Application***

Authors: Crystal M. Cook and John M. Haake

Heat treating: Proceedings of the 20<sup>th</sup> conference: Volume 1 & 2  
20<sup>th</sup> ASM Heat Treating Society Conference Proceedings, 9-12 Oct., 2000, St. Louis, MO, ASM international, 2000

## **Abstract**

HPDDL surface transformation hardening can be used to either harden localized portions of a part, or the user may scan side by side to yield and unlimited surface hardened width. In this experiment surface transformation hardening was performed on ferrous materials to determine the advantages of temperature control and monitoring in a HPDDL system with a pyrometer and thermal imaging system.

## **Introduction/Background**

Surface hardening is used to extend the versatility of certain metals by producing combinations of properties not readily attainable in other ways. For many applications, wear and the most severe stresses act only on the surface of the part. Therefore, the part may be surface hardened by a final treatment after all other processing has been accomplished including the last machining step. Laser surface hardening techniques may be used in situations where the surface of the part needs to be hardened without changing the bulk composition of the part. The flexibility of laser delivery systems, low distortion and high surface hardness have made lasers prevalent in applications that require selective hardening of wear and fatigue prone areas of machine components<sup>1</sup>.

A comparison with flame and induction surface transformation hardening techniques clearly show that laser surface hardening is the most advantageous process. Flame hardening has poor reproducibility, poor quench and environmental issues. In induction hardening a quench is required, distortion of the part occurs

and there is large thermal penetration. A comparison with carburizing, nitriding and carbonitriding techniques also indicates advantages of laser surface processing. In pack carburizing processes it is difficult to control case depth. Whereas liquid carburizing can pose disposal problems with the salt bath and the baths often require frequent maintenance. Nitriding can be used to produce parts with high hardness and low distortion. A laser surface transformation hardened part can be produced with a deeper case and similar case hardness to that of a nitrided sample. Gas carbonitriding produces parts with less distortion than carburized parts, however gas control is critical in this process<sup>2</sup>. With laser beam hardening the applied light radiation instantaneously heats the surface, there is no radiation spillage outside the optically defined area. The bulk of the material acts as a heat sink for the extraction of heat from the surface, therefore a quench is not required<sup>3</sup>. The major advantage of laser surface treatment is high processing speeds with precise case depths. Laser surface transformation hardening does not require an atmosphere and is environmentally friendly. Laser surface transformation hardening not only increases the wear resistance, but also under certain conditions the fatigue strength is also increased due to the compressive stresses induced on the surface of the component<sup>3</sup>. The HPDDL is an ideal source for laser surface transformation hardening. The line of light, when moved across the work piece along the short axis has high edge definition without the need for special cylindrical lenses [Nd:YAG] or water cooled integrators [CO<sub>2</sub>]. The wavelength is 800nm, which is highly absorptive and does

not require pre-coating of the work piece. The ISL-4000L has a modulation bandwidth of 20KHz, making ideal for in-situ temperature control.

There are many parameters that determine the effectiveness of a laser surface hardening treatment. The primary processing parameters used to obtain the experimental data are; laser power, processing speed, and beam profile. An increase in the laser power will result in a dramatic increase in the depth of hardening. An increase in processing speed will result in a decrease in the case depth. The beam profile [width] is a necessary criterion in the determination of the degree of surface hardening that may take place. The hardness data obtained from the experimental runs will provide information about the degree of hardening and case depth. The microstructures produced by the heat treatment should also be considered to determine if the surface treatment is successful. The processing temperature, quench time and final temperature of the part must also be carefully monitored to ensure that the surface of the part is properly austenitized and that a proper cooling rate occurred.

**Surface Transformation Hardening** A key application for this laser is surface transformation hardening. This laser was designed with this application in mind. The laser provides a line beam with dimensions of 12 mm X 1mm FWHM at focus. This beam which has a top hat profile along the 12 mm direction can be swept over the surface to produce the desired hardening. Because of the large area covered directly by the beam, this laser can quickly and uniformly treat large parts.

Laser surface transformation hardening is the heating of a surface by use of a laser followed by the rapid quenching of the surface by heat conduction into the part. This provides a hardening on the surface of the material through a solid-state transformation that results in the formation of a high-hardness microstructure, i.e. martensite. Varying the amount of heat input provided to the work-piece may alter the depth

of the hardened zone. In this evaluation, varying travel speed altered heat input. During these evaluations, the length dimension of the spot of focus, which was approximately 0.47” to 0.55” (12 to 14 mm), was directed perpendicular to the direction of processing. This allows very large surface areas to be hardened in a single pass. Laser surface transformation hardening is often used to harden localized areas of machine components such as gears and bearings. A flat-topped shaped hardened zone is obtained through a laser beam surface treatment.

**Absorption Efficiency** The HPDDL used in this study generally operates with a center wavelength of 810 nm, which is in the near infrared range and not visible to the human eye. Typically, direct diode lasers operate at a shorter wavelength than the Nd:YAG [1.06 um] and CO<sub>2</sub> [10.6 um] lasers, which are commonly used in industrial applications. This leads to an advantage of the diode laser system, since the lower operating wavelength results in a higher absorption rate with most metals<sup>4,5</sup> [Figure 1]. Laser transformation hardening of steels is typically performed with a CO<sub>2</sub> laser but the parts need to be coated with absorptive coatings for the otherwise reflective surface. These coatings are involve significant costs added to the laser hardening process. In addition, these coating are notoriously inconsistent during the dynamic hardening process. Users can experience significant cost savings by eliminating the absorption coating process. Additionally, the use of the HPDDL process is more environmentally friendly; disposal of waste paint, clean-up consumables, elimination of air-born particulate, VOC and air filters are eliminated. Like the HPDDL the Nd:YAG the lasers also do not require coatings but there are limits to the fiber delivery and beam shaping systems. Large components require continuous beam-on times in excess of 30 minutes at full power to cover the required surface area; thus requiring special cooling.<sup>6</sup> The HPDDL does not require fiber optics the beam, which is naturally a line of light, is directly applied to the work piece.

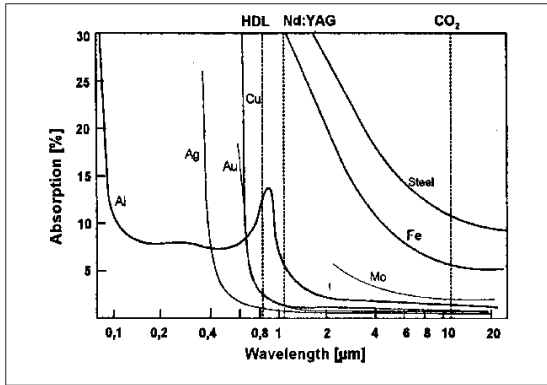


**Figure 1 - Absorption vs. Wavelength for typical metals**

**Operating Costs** The advantages of the HPDDL are their high electrical to optical conversion efficiency. The laser diodes used by Nuvonyx have demonstrated electrical to optical conversion efficiencies as high as 60%. The net result is a laser system with a wall plug electrical to optical power conversion efficiency of >25%. Consequently, a 4,000 Watt CW laser diode system consumes less than 16,000 Watts of electrical power, including the laser water-cooling system. This efficiency translates into a lower cost of operation for the user and a much smaller footprint as shown in Table 1.

	DIRECT DIODE ISL	CO2 FLOWING	Nd:YAG FLASH PUMPED	Nd:YAG DIODE PUMPED
Net system efficiency, %, continuous operation at 100% power, including chiller	25%	6%	1%	6%
Hourly operating cost, \$, continuous operation at 100% power	\$1.50	\$10.00	\$30.00	\$6.00
Wave Length, um	0.8	10.6	1.06	1.06
Absorption % - steel*	40%	12%	35%	35%
Absorption % - Aluminum*	13%	2%	7%	7%
Average intensity	10 <sup>3</sup> to 10 <sup>6</sup> constant	10 <sup>3</sup> to 10 <sup>3</sup> constant	10 <sup>3</sup> to 10 <sup>7</sup> constant	10 <sup>3</sup> to 10 <sup>7</sup> constant
Current maximum power (kW) commercially available	4	50	4	4
Footprint for laser, power supply, chiller, sq. ft.	8 sq. ft.	50 sq. ft.	100 sq. ft.	60 sq. ft.
Replacements, hours	Laser Arrays, 10,000 hrs	2,000hrs, Blower/Turbine - 20-30,000 hrs	Lamps - 1,000 hrs	Pumping Arrays - 10,000 hrs
Laser/Beam Mobility	High/High	Low/Medium	Low/High	Low/High
* Higher absorption means less reflected energy, and more efficient use of the laser beam				

**Table 1- Operating costs for commonly used industrial lasers**

**Solid State Advantage** Another advantage of direct diode lasers is that they are solid-state lasers. This yields a highly controllable heat source. Power can also be turned on and off instantaneously. The instantaneous power control of the HPDDL realizes significant energy savings. The HPDDL laser demonstrated in this study is microprocessor controlled and has a

modulation bandwidth of 20KHz. This is an order of magnitude higher than conventional lasers. Unlike conventional systems, diode lasers do not require warm up time to stabilize. The limitation in the feedback control is no longer the laser but the temperature monitoring systems. The pyrometer used in this experiment has 1000Hz response. The thermal camera has a 600Hz response, this is the limitation in the control network.

Infrared temperature sensors or pyrometers measure the surface temperature of objects without contact. The sensor work based on the principle that the energy emitted by an object is proportional to its temperature. Like a camera, the sensors use an optical system to collect the radiant energy emitted by the measured target. This energy is focused on an infrared detector that provides an output signal which varies with the intensity of the energy. This signal is then processed by the sensor electronics to provide the desired temperature output. This temperature output can be displayed on a digital meter, or it can be in the form of a current or voltage output signal that varies linearly with temperature. These temperature output signals can then be input into a computer, controller, or other device for process monitoring and control.

The particular units used here is a fiberoptically couple single wavelength [0.9 microns] infrared temperature sensor. Single wavelength temperature sensors measure the amount of energy emitted by an object within a specified infrared spectral band, or operating wavelength. Since the energy emitted by an object is a function of both emissivity and temperature, the single wavelength sensor measures the energy and assumes a constant preset emissivity value to calculate the remaining unknown variable, temperature. The single wavelength sensors are the most common type of sensor with the largest selection of options for temperature range, optics, wavelength, and response time. There are sensors available to measure temperatures ranging from -50 to 4500F (-45 to 2500C). While single wavelength sensors can be used for most applications, they must be used properly in order to achieve accurate and repeatable results.

Thermal imaging works on the same principles as pyrometry. Modern CCD's and scanning CMOS devices are quite stable over time and each pixel of these cameras can be calibrated as a separate pyrometer. The primary

advantage of thermal imaging is that temperature can be measured in two dimensions rather than at a single spot. Thermal imaging yields information on the temperature of each pixel, as well as the spatial distribution of temperature. In many measurement situations there are invariably thermal gradients. Thermal imaging allows the user to visualize these gradients.

With the computational power of a PC, it is possible to capture thermal images at high rates of speed, process this information, record thermal data for analysis, and provide feedback control of temperature in real time. The processing provides the temperature at any location, the area at a given temperature, and the rate of change of temperature with distance (and time). Thermal imaging can also be used to verify process conditions. We use a digital camera of 128x128 pixels that operates at a frame rate of 490Hz. The frames are transferred to the PC with IEEE 422 cable to a frame grabber operating on the PCI bus. With LabView software it is possible to run a control loop at 100Hz in a PC environment. Faster rates are possible with hard coded systems.

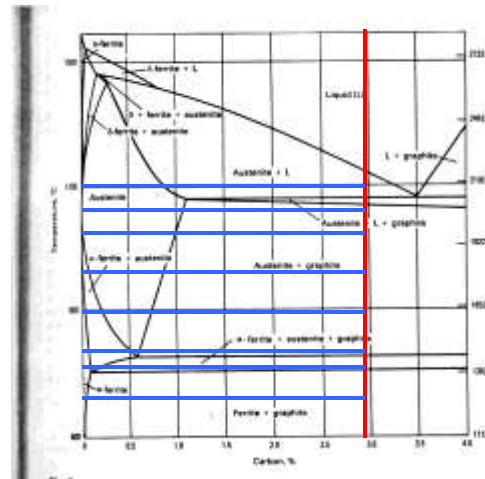
### Experimental Data

**Experimental Procedure** Preliminary research was performed to relate the amount of backtemper to the displacement of the beam along the long axis. Three pieces of 4140 steel with a length of 304.8 mm, width of 50.8 mm and thickness of 12.7 mm were surface hardened in varying ways. The process speed, power and the amount the beam was defocused were kept constant throughout the experimentation. The displacement of the beam along the long axis varied from 12 to 20 mm in 0.5 mm increments.

Pyrometer controlled runs were done on 4140 steel as well as Class 40 Gray Cast Iron. The process speed was at 0.5 m/min, the surface temperature of the part was monitored by a pyrometer and the output power was controlled to maintain a constant temperature on the part. A phase diagram was used to choose the various set temperatures for the surface hardening

operation [Figure 2]. The red [vertical] line on the phase diagram shows the approximate carbon content of the 4140 steel samples; the green [horizontal] lines are the specified process temperatures. Gray cast iron had a similar experimental schedule.

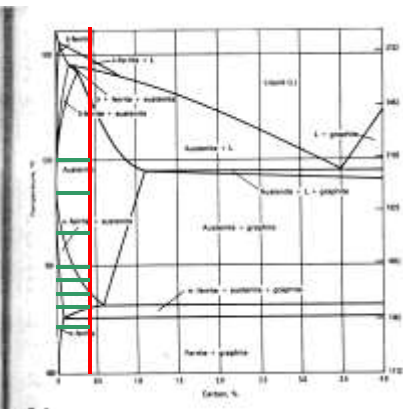
**Figure 2: Phase diagram indicating process temperatures for 4140 steel.**



**Figure 3: Phase diagram indicating process temperatures for the gray cast iron runs.**

Temperature monitoring was also performed with a thermal imaging system. Each hardened pass was produced at a power of 4kW; the process speed was varied for each run. The beam width was kept constant for each sample. The data collected from the thermal imaging system was for the cooling rate and gradient analysis.

Both the thermal imaging and pyrometer samples were metallographically prepared. Microhardness measurements were taken on each sample [Figure 4] to determine the depth of the hardened case. Five case depths measurements were taken on each sample to determine the uniformity of the case. The first case measurement was taken in the middle of the case, respective measurements were taken at 2 and 4 mm from the center of the pass. Microstructural analysis was also performed on each sample.



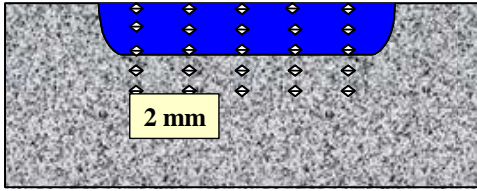


**Figure 4:** Sketch of a part that has been analyzed through microhardness.

**Preliminary Research** The optimum results with regard to back-temper, surface hardness and case depth were obtained by making a single pass by the laser, quenching, then moving the beam over 14.5 to 15.5 mm. The minimum back-temper reading for two passes at a given displacement was found to be 15 mm. The hardness within the case was found to be in the range of 50 to 65 R<sub>c</sub>, while the case depth was generally between 0.7 and 1.5 mm. The hardness and case depth can be controlled by the input power and travel speed of the beam. Through experimental data, the width of the laser beam is approximated at 14 mm.

Samples have been produced with a case depth of 1.5 mm, however the average case depth observed was 0.8 mm (Figure 5). The hardness in the case is generally in the range of 50 to 65 R<sub>c</sub>. The hardness as well as the case depth can be controlled to some degree by the power input and travel speed.

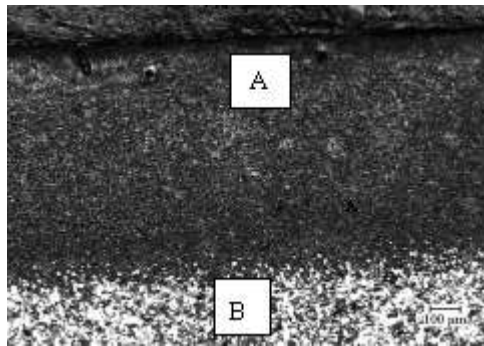


**Figure 5:** A sample with a case depth of 0.8 mm. The phase labeled A is the surface hardened martensite; the phase labeled B is the base metal, which is composed of pearlite and ferrite

Microscopic analysis was done on the passes made at displacements of 14.5, 15.0 and 15.5 mm. The microscopic analysis showed a back-tempered region in samples in which the beam was displaced 15.5 mm or less. This occurs because the part is held in the tempering temperature range (most likely above 425 C) for

a short time. Since the sample is held in this high temperature tempering range for a short time, there is usually a drop in hardness to 30 to 40 R<sub>c</sub>. [Figure 6] A martensitic structure results in high strength, wear resistance and hardness. Tempering the martensite will result in a decrease in the brittleness and an increase in the toughness. In order to determine the amount of backtemper the microhardness was taken in the overlapping pass region. A case depth of 0.5 mm was assumed to determine the amount of backtemper in a sample. In some cases the back-tempered region can be as wide as 5 mm in the region between the first pass made by the laser and second pass, however this only occurs when two passes are overlapping. The amount of back-temper observed in a sample can be controlled and reduced to 1.5 mm or less by controlling shifting the beam 15 mm along the long axis for the given power density and beam width parameters.

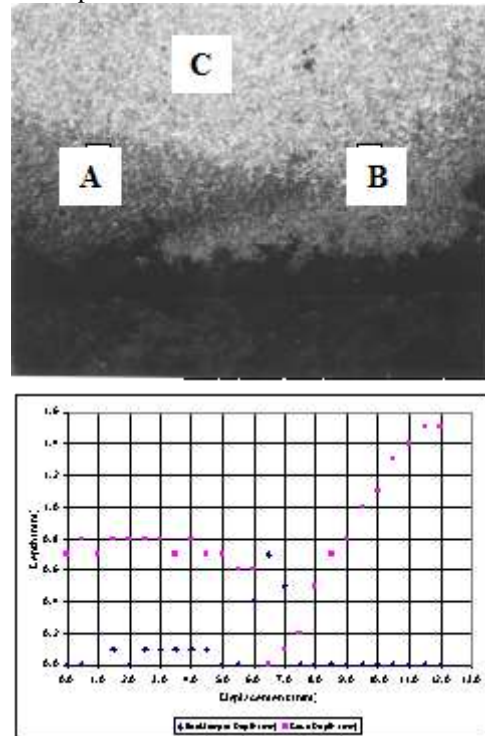


**Figure 6:** This sample was produced by shifting the beam 15 mm from the initial pass to produce the second pass. The region marked A is untempered martensite. B marks the region in which the martensite is tempered. C indicates the base metal (2% Nital etch, 50X magnification).

Relatively high hardness values are consistent throughout the case. Figure 7 shows the hardness distribution for the case of the second

pass made by the laser at a displacement of 15 mm. The depth of the case for this sample was found to be 1.5 mm. The case hardness is in the range of 51.8 to 67.2 R<sub>c</sub>. The gray portion of the graph indicates that the hardness within the case is in the acceptable range.

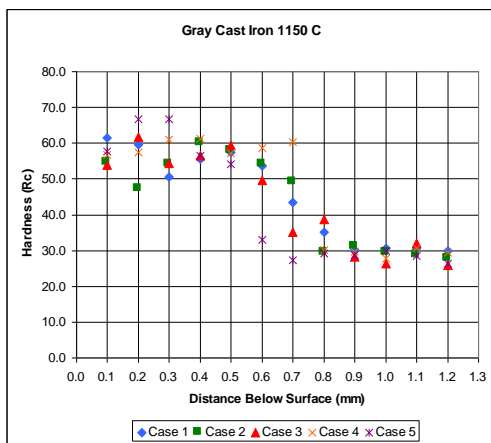


**Figure 6: Hardness distribution for a sample produced by moving the beam 15 mm from the initial pass.**

**Temperature Control with a Pyrometer**  
 Temperature control can easily be integrated into the ISL 4000L system due to a 20 kHz bandwidth. The use of a pyrometer enables the user to predict the microstructural characteristics of a sample by choosing an appropriate temperature to produce martensite. The signal of the pyrometer is monitored and the output power of the laser is adjusted to maintain a constant temperature. A screen printout from a pyrometer controlled run shows readings for surface temperature of the part and output laser power [Figure 7].



**Figure 7: Printout of pyrometer controlled hardening pass produced on gray iron at 1000°C.**

The depth of the hardened case as well as the hardness within the case is controlled by the width of the beam. As the width of the beam increases the case depth will typically increase, however, the hardness within the case will decrease. A beam width of 2 mm was chosen for the 4140 steel runs, while a beam width of 6 mm was used in processing the class 40 Gray Cast Iron.

The microstructure of the gray cast iron resulting from the pyrometer controlled run at 1150°C indicates that at this temperature melting does not occur. A visual examination of the heat-treated pass confirms this observation [Figure 8]. Melting would be expected at this temperature, the phase diagram indicates that this sample would be in the L +  $\gamma$  region. However, in cast irons the amount of silicon in the sample determines the hardenability of the part, the phase diagram shown in Figure 3 is the iron carbon phase diagram at 2.5% Si. Class 40 gray iron has only 1.70 to 2.00% silicon. This could be the reason the phase diagram does not correlate with the 1150°C reading at 1200°C melting does occur, as expected from the phase diagram. The case depth of the sample produced at this temperature is 0.6 mm, the hardness within the case is between 50 and 60 Rockwell C. [Figure 9]



**Figure 8: Microstructure of Gray Cast Iron sample that was produced at a surface temperature of 1150°C.**

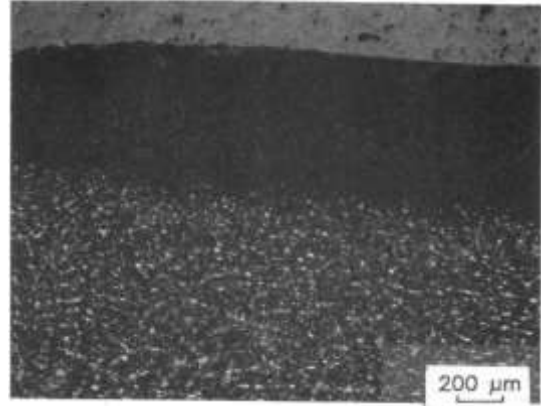


**Figure 10 Microstructure of 4140 steel sample that was produced at a surface temperature of 1100°C - 50X**

A comparison of the results with the known data indicates that the cast iron temperature monitoring is very effective. A direct correlation with the phase diagram can be made in comparing the cast iron case depth, temperature reading and phase diagram. However, the 4140 steel case depth data does not seem to correlate with any known data. This might be due to the emissivity difference or change of emissivity during processing of the 4140 as compared to the cast iron the cast Iron.

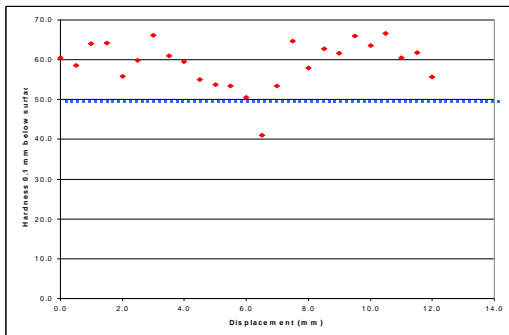


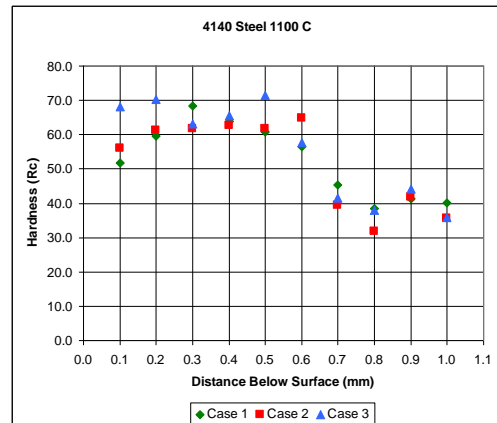
**Figure 9 Microhardness from 1150C Grey cast Iron -Pyrometer controlled**

The 4140 steel at a controlled surface temperature less than 1100°C hardening is not observed and the microstructure is composed of ferrite and pearlite. At a temperature of 1100C a martensitic case is visible. [Figure 10] The base metal is ferrite and pearlite. At a surface temperature of 1100°C a case depth of 0.6 mm is observed. The hardness within the case is between 50 to 70 RC. [Figure 11].

**Figure 11 Microhardness from 1100C 4140 pyrometer controlled**

### Thermal Imaging

*Visual Analysis* A visual analysis of the 4140 steel heat treating pass produced at 1.75 m/min indicates that there are melt oscillations on the heat treated pass. [Figure 12] These oscillations



are uniform and were recorded for future

analysis. Thermal imaging data allow us to do a simple set of experiments for each sample to achieve the optimum case depth and find the spot between the melting and martensite formation. This can also be used to calibrate a pyrometer without the use of fuzzy variables such as emissivity of the material being heat-treated. These oscillations occur because as you drive the temperature up by lowering the process speed, the heat of fusion puts a delay between when the heat is applied and the response of the part. These self-oscillations will occur for any material.

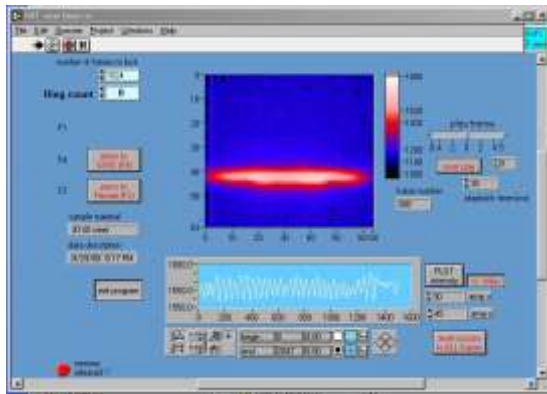


**Figure 12 Thermal imaging and analysis**  
*Cooling Rate Analysis.* The cooling rate observed from the thermal imagery is lower than that reported through earlier analysis. There is a dip in the cooling rate at the melt transition area. [Figure 13]

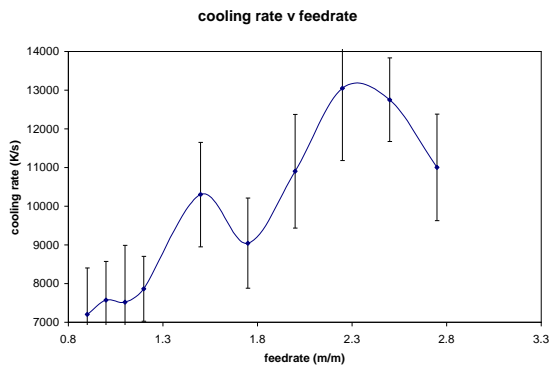
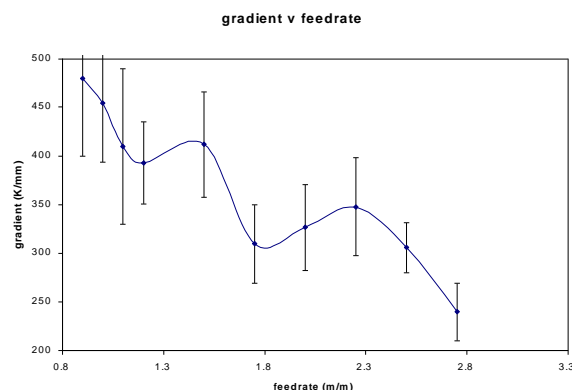


**Figure 13 Cooling Rate vs. feedrate on 4140 steel**

A dip in the gradient is also evident in the melt/ non-melt transition area [Figure 14]. The



gradient is dampened by the heat of fusion at approximately 1.75M/min.

**Figure 14 Gradient vs. feed rate for 4140 steel**  
*Case Depth Data* A dip in the case depth is also observed in the transition zone of the 4140 steel samples. This appears to correlate with the thermal imaging data where a phase change is evident at 1.75 m/min. [Figure 15]

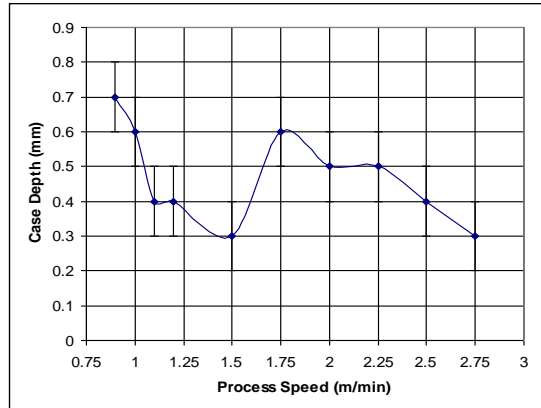


**Figure 15 Case Depth vs. Process speed**

*Microstructural Analysis* At a low process speed melting is observed in the cast iron samples. Microstructural changes associated with laser melting are in the form of grain refinement, solid solutions, and fine dispersions of precipitates. In the melt zone of the gray iron dendritic ledeburite with small amounts of plate like, high carbon martensite and retained austenite is formed. Below the melt zone is the heat affected zone which appears lighter in contrast this region is comprised of interdendritic flake graphite with ferrite dendrites [Figure 14].

The microstructures in un-melted gray iron samples correlated with earlier research that indicates that the case is comprised of sequential regions with varying degrees of microstructural modification<sup>7</sup>. The region below the melt zone contains plate martensite, retained austenite and graphite. The region near the base metal is comprised of interdendritic flake graphite, refined martensite and untransformed pearlite.

The 4140 steel samples consisted of a martensitic case, the unhardened area was composed of ferrite and pearlite.<sup>7</sup>

## 5.0 Conclusions

HPDDL systems are versatile laser systems capable of meeting the needs of many current heat treating applications. The advantages of direct diode lasers are the high wall plug

Presented at the 20<sup>th</sup> ASM Heat Treating Society Conference Proceedings October 9-12, 2000 in St. Louis, MO

efficiency, order of magnitude smaller footprint, lower maintenance, high absorption in work piece, and high control bandwidth. The benefits of the unique beam properties and 800nm wavelength of the ISL-4000L HPDDL and its benefits have been demonstrated. Further taking advantage of the line source and processing along the short axis, large area heat-treating is possible. Laser hardening experiments were successfully conducted on 4140 steel and gray cast iron without the need for pre-coating. Preliminary studies indicate that backtemper is minimized through the use of a HPDDL system. High case depths can be achieved by controlling the width of the beam.

Temperature control is enabled by the solid state nature of HPDDL. Surface temperature control was demonstrated with the use of a pyrometer. Prediction of the microstructure formed was demonstrated through the use of temperature control.

Thermal Imaging indicates that the gradient and cooling rate are dampened by the heat of fusion. The uniform laser beam profile imaged correlates with a uniform case depth of more than 0.5 mm.

Future work will take advantage of fact that HPDDL inherently provide the ability to control the output laser energy with a degree that is unmatched by conventional Nd:YAG and CO2 lasers, allowing for the study of the phase transition regions in metal work pieces.

## 6.0 References

1. G. Krauss, *Steels – Heat Treatment and Processing Principles*, pp 339-345, ASM International, Materials Park, Ohio (1990)
2. *Advanced Materials and Processes, Heat treating and coating*, Vol 156 No. 6 p 149
3. N. B. Dahotre, *Laser in Surface Engineering*, pp 70-86, ASM International, Materials Park, Ohio (1998)
4. E. Schubert et al., “New Possibilities for Joining by Using High Power Diode Lasers”, LAI Proceedings ICALEO’ 98, VOL 85
5. Handbook of chemistry and Physics, 64th edition 1983-1984 , CRC press
6. J. Koch and L. Maass, *Industrial Laser Solutions*, August 2000, pp.7,9,&11.
7. *Cast Irons*, ASM International, Materials Park, Ohio (1996)